Title

Mechanosensitive Control of Articular Cartilage and Subchondral Bone Homeostasis in Mice Requires Osteocytic Transforming Growth Factor β Signaling

Journal

Arthritis & Rheumatology, 73(3)

ISSN

2326-5191

Authors

Bailey, Karsyn N
Nguyen, Jeffrey
Yee, Cristal S
et al.

Publication Date

2021-03-01

DOI

10.1002/art.41548

Peer reviewed

Published in final edited form as:

Arthritis Rheumatol. 2021 March ; 73(3): 414–425. doi:10.1002/art.41548.

Mechanosensitive Control of Articular Cartilage and Subchondral Bone Homeostasis Requires Osteocytic TGFβ Signaling

Karsyn N. Bailey[1,2], **Jeffrey Nguyen**[1,3], **Cristal S. Yee, PhD**[1], **Neha S. Dole, PhD**[1], **Alexis Dang, MD**[1,4], **Tamara Alliston, PhD**[1]

[1]Department of Orthopaedic Surgery, University of California San Francisco, San Francisco, CA

[2]UC Berkeley-UCSF Graduate Program in Bioengineering, San Francisco, CA

[3]Department of Biomedical Engineering, California State University, Long Beach, Long Beach, CA

[4]San Francisco Veterans Affairs Medical Center, San Francisco, CA

Abstract

Objective: TGFβ signaling plays a complex tissue-specific and non-linear role in osteoarthritis (OA). We sought to identify the osteocytic contributions of TGFβ signaling to OA.

Methods: To uncover the role of osteocytic TGFβ signaling in joint homeostasis, we used 16-week-old male and female mice with an osteocyte-intrinsic ablation of TGFβ type II receptor (TβRII$^{ocy-/-}$) and assessed defects in cartilage degeneration, subchondral bone plate (SBP) thickness, and SBP sclerostin expression. To further investigate these mechanisms in 16-week-old male mice, we perturbed joint homeostasis using the medial meniscal/ligamentous injury (MLI) model at 8 weeks of age, which preferentially disrupts the mechanical environment of the medial joint to induce OA.

Results: In all contexts, independent of sex, genotype, or medial or lateral joint compartment, increased SBP thickness and SBP sclerostin expression were spatially associated with cartilage degeneration. Male TβRII$^{ocy-/-}$ mice, but not female TβRII$^{ocy-/-}$ mice, have increased cartilage degeneration, increased SBP thickness, and higher levels of SBP sclerostin, demonstrating that the role of osteocytic TGFβ signaling on joint homeostasis is sexually dimorphic. With changes in joint mechanics following injury, control mice increase SBP thickness, subchondral bone volume, and SBP sclerostin expression. TβRII$^{ocy-/-}$ mice, however, are insensitive to subchondral bone changes with injury, suggesting that mechanosensation at the SBP requires osteocytic TGFβ signaling.

Conclusion: Our results provide new evidence that osteocytic TGFβ signaling is required for a mechanosensitive response to injury, and that osteocytes control SBP homeostasis to maintain cartilage health, uncovering osteocytic TGFβ signaling as a novel therapeutic target for OA.

Corresponding Author: Tamara Alliston, PhD, University of California San Francisco, Department of Orthopaedic Surgery, 513 Parnassus Avenue, S1155, San Francisco, CA 94143, 1-415-502-6523, Tamara.Alliston@ucsf.edu.

Conflicts of interest: All authors: none.

Introduction

Osteoarthritis (OA), considered a “whole joint” disease, is characterized by the irreversible disruption of multiple joint tissues including articular cartilage and subchondral bone (1). While the relationship between cartilage degeneration and subchondral bone changes is an established hallmark of OA, the causal mechanisms driving the coordinated loss of homeostasis in these two tissues remains unclear. The subchondral bone plate (SBP), for example, undergoes dynamic remodeling in OA, with thinning and increased remodeling in early joint disease and thickening spatially associated with cartilage degeneration in late-stage OA (1–7). SBP changes can impact both the mechanical and biological environment of the joint. Given its proximity to the articular cartilage, the SBP can impact the stress concentration at the articular cartilage during joint loading (2), which is one possible explanation for the spatial association of SBP thickening and cartilage degeneration. Additionally, the SBP acts as a physical boundary, regulating cartilage exposure to vasculature, oxygen, nutrients, and cytokines (1). During OA progression, the SBP becomes permeabilized with increased vascular invasion, disrupting the homeostatic biological environment and aggravating cartilage degeneration (1). While SBP thickening is considered an indisputable sign of late-stage OA, the underlying mechanisms of the thickening are still largely unknown, and whether it contributes to or is the consequence of cartilage degeneration remains elusive.

The transforming growth factor beta (TGFβ) signaling pathway plays an important role in both bone and cartilage homeostasis, and imbalanced TGFβ signaling results in disease in each tissue, such as osteogenesis imperfecta in bone (8) and OA in cartilage (9–11). TGFβ signaling is critical for maintaining bone mass and quality (12–15) and balanced TGFβ signaling in each tissue compartment is integral for joint health. In some contexts, TGFβ signaling protects against OA (9–11, 16–19), and in other contexts TGFβ signaling exacerbates OA (20, 21). Two key concepts clarify the sophisticated function of TGFβ in joint homeostasis. First, TGFβ action in the joint is tissue compartment- and cell type-specific. Second, the effect of TGFβ on the joint is non-linear, such that an optimal level of signaling is required for joint homeostasis, and highly active, suppressed, or imbalanced canonical and non-canonical TGFβ signaling drives joint degeneration. More specifically, loss-of-function mutations in the canonical TGFβ effector SMAD3 increase the incidence of OA in humans (16, 18) and in mice (9–11). In the absence of chondrocyte-intrinsic Smad3, TGFβ signaling activates non-canonical pathways that prevent cartilage anabolism and stimulate MMP13-dependent cartilage catabolism (9–11). Conversely, systemic inhibition of TGFβ signaling in mice has been shown to exert dose-dependent benefits on joint health, in part, by suppressing TGFβ signaling within mesenchymal stem cells (MSCs) (20, 21). Taken together, this further emphasizes the need to uncover the precise role of TGFβ signaling in each joint tissue to maintain homeostasis.

The role in OA of TGFβ signaling in bone cell types is less well-defined. Although osteocytes participate in human and mouse OA (22), the role of osteocyte-intrinsic TGFβ signaling in joint homeostasis is unknown. In addition to coordinating the flow of nutrients through the canalicular network and regulating the mechanosensitivity of bone, osteocytes may also impact cartilage through a process known as perilacunar/canalicular remodeling

(PLR) (23). During PLR, osteocytes secrete acid and proteases to dynamically resorb and then replace their surrounding bone matrix to maintain the mineral homeostasis, the canalicular network, and bone quality (24–27). Osteocyte-intrinsic inhibition of TGFβ signaling causes PLR suppression, including disrupted canalicular networks, dysregulation of PLR enzyme expression, increased trabecular bone volume, and inferior bone quality in male, but not in female, mice (23, 28). Thus, osteocytic TGFβ signaling functions to maintain both biological and structural properties of bone, each of which could impact cartilage integrity. Combined with the known role of TGFβ signaling in skeletal mechanobiology (29–32), osteocytic TGFβ signaling may contribute to joint homeostasis through a number of mechanisms.

To dissect the osteocyte-specific contributions of TGFβ signaling on joint homeostasis, we tested the hypothesis that loss of osteocytic TGFβ signaling exacerbates OA through its control of subchondral bone. Our findings reveal that osteocytic TGFβ signaling is critical for cartilage health, SBP homeostasis, and mechanosensitive response to injury, elucidating a new mechanism of bone-cartilage crosstalk.

Materials and Methods

Mice

To assess the role of osteocytic TGFβ signaling in joint homeostasis, mice were bred to generate $T\beta RII^{ocy-/-}$ mice (DMP1-Cre^{+}; $T\beta RII^{fl/fl}$) and littermate control mice (DMP1-Cre^{-}; $T\beta RII^{fl/fl}$) (23, 28). Animals were housed in groups in a pathogen-free facility at 22°C with a 12-hour light/dark cycle and supplied with standard irradiated mouse chow and water ad libitum. The Institutional Animal Care and Use Committee (IACUC) at the University of California San Francisco approved all animal procedures.

For the basal joint phenotype, hindlimbs were collected from 16-week-old control and $T\beta RII^{ocy-/-}$ male and female mice (n=7-11 mice per group). To analyze the effect of joint injury, male control and $T\beta RII^{ocy-/-}$ mice (8 weeks) were subjected to bilateral sham or meniscal-ligamentous injury (MLI) surgery, as described (n=9-11 mice per group) (33). Under sterile conditions and in isoflurane-anesthetized mice, incisions were made through the skin and joint capsule medial to the patella, and the medial collateral ligament (MCL) was transected and the medial meniscus was removed. Sham-injured animals received bilateral incisions without MCL transection or meniscal removal. Incisions were closed with sutures, and animals received an injection of long-acting buprenorphine analgesic. Hindlimbs were collected 8 weeks post-surgery.

MicroCT Analysis

A 4-mm region of the left hindlimb, centered on the joint, was scanned using a Scanco μCT50 specimen scanner with an X-ray potential of 55 kVp, current of 109 μA voxel size of 10 μm, and integration time of 500 milliseconds. Thresholding was performed as described (22, 23, 34).

The tibial plateau subchondral bone region was designated 200 μm from the proximal surface of the tibia to exclude the subchondral bone plate (SBP) and extended 250 μm

distally. Contours were delineated by a blinded reviewer at the periosteal surface with a linear boundary bisecting the medial and lateral halves, and bone volume fraction (BV/TV) was reported.

The femoral SBP was contoured in a blinded manner in sagittal microCT images of the femoral condyles. Femoral SBP thickness, rather than tibial SBP thickness, was analyzed because tibial SBPs were too thin and too close to the growth plate for meaningful analysis (7). For quantification, circles of diameter 750 μm were consistently placed on grayscale 3D thickness maps, centered on the lateral anterior, medial anterior, lateral posterior, and medial posterior regions, as described (7), and mean pixel intensity was measured. Pixel intensity was converted to SBP thickness in μm (n=9-10 mice per group). Representative grayscale images were converted to pseudocolor for illustration in figures.

Qualitative differences in shape between control and TβRII$^{ocy-/-}$ mice were identified by a blinded grader on 2D sagittal images of the knee, using cross-section of the patella as a landmark (n=7-11 mice per group).

Histology

Right hind limbs were paraffin-embedded at 90 degrees of flexion in the coronal orientation and sectioned at 6 μm thickness. Brightfield images were acquired on a Nikon Eclipse E800 microscope, and fluorescent images were acquired on a Leica DMi8 confocal microscope.

Immunofluorescence (IF) was used to identify cells expressing TβRII or sclerostin in the subchondral bone and articular cartilage of the knee. Sections (6 μm) were incubated with primary antibodies: rabbit anti-TGF beta Receptor II antibody (1:500 for male mice, 1:250 for female mice, Abcam ab186838), goat anti-SOST/Sclerostin (1:200, R&D Systems AF1589), or species-specific non-immune IgG negative controls. This was followed by incubation with secondary antibody conjugated to Alexa Fluor 594 (for TβRII: goat anti-rabbit 1:1000, Invitrogen AB_2534079; for sclerostin: donkey anti-goat 1:1000, Invitrogen AB_2534105). Positively-stained cells were counted by a blinded grader in 20x visual fields from each joint quadrant using ImageJ and reported as % positive cells in each respective tissue (n=4-8 mice per group).

The osteocytic lacunocanalicular network was visualized using the Ploton silver stain with a Cresyl Violet counterstain, and articular cartilage was visualized using the Safranin-O/Fast Green stain. Sections (6 μm) were selected from the mid-joint region using the identification of the ACL and PCL as landmarks and stained, as described (22, 23, 35, 36).

For subchondral bone mean canalicular length, four images per joint quadrant at 100x visual field were acquired, and length was quantified in a blinded manner using ImageJ by tracing 10 canaliculi per osteocyte and three osteocytes per image (48 osteocytes per animal, n=5 mice per group). Canalicular lengths were averaged to obtain a mean canalicular length for each sample, and mean lengths were averaged and reported for each group.

For OA score, each joint quadrant (medial tibia, lateral tibia, medial femur, lateral femur) was imaged and graded by three blinded graders using modified Mankin (37) and OARSI (38) grading schemes (n=9-11 per group). Scores from all graders were averaged to obtain a

mean score, and mean scores were then averaged within each group. Total score represents the sum of all four quadrants.

Statistical Analysis

Comparisons between genotypes, for male and female mice, were tested using an unpaired two-tailed Student's t-test. Comparisons among genotype and injury employed two-way ANOVA followed by Tukey post-hoc tests. Statistical analyses were performed in GraphPad Prism 8 (GraphPad Software, Inc.). Values are expressed as mean ± SD for outcomes reporting a mean of individual measurements or ± SEM for outcomes reporting a mean of mean measurements. P-values less than 0.05 were considered statistically significant, with sample size "n" specified in figure legends.

Results

Requirement of osteocytic TβRII for subchondral bone canalicular homeostasis

To determine the specificity of the DMP1-Cre promotor in the joint, we evaluated the expression of TβRII in control (DMP1-Cre^{-};TβRII$^{fl/fl}$) and TβRII$^{ocy-/-}$ (DMP1-Cre^{+};TβRII$^{fl/fl}$) knees. Relative to a control non-immune IgG, immunofluorescence revealed TβRII expression throughout the meniscus, cartilage, subchondral bone, and bone marrow of control mice (Figure 1A, 1C). A blinded semiquantitative analysis of TβRII expression in subchondral bone osteocytes revealed a significant 38% decrease between control and TβRII$^{ocy-/-}$ male mice, with no change in percentage of TβRII-positive articular chondrocytes (Figure 1B) or in osteocyte density. This selective disruption of TβRII in subchondral bone allows us to evaluate the role of osteocytic TGFβ signaling in joint homeostasis.

We have previously reported that male TβRII$^{ocy-/-}$ mice demonstrate osteocyte perilacunar/canalicular remodeling (PLR) suppression within the axial femur, with reduced expression of several essential PLR enzymes and a corresponding reduction in canalicular length (23, 28). We evaluated the effect of osteocyte-intrinsic TβRII-deficiency on canalicular length in subchondral bone. TβRII$^{ocy-/-}$ mice exhibit a significant reduction in canalicular length within the subchondral bone of the tibial plateau and femoral condyles compared with control mice at 16 weeks of age (Figure 1D, 1E). In our model of an osteocyte-specific loss of TGFβ signaling, we find evidence of impaired PLR in the subchondral bone of male TβRII$^{ocy-/-}$ mice.

Requirement of osteocytic TβRII for cartilage homeostasis is sexually dimorphic.

Given the evidence for osteocyte dysfunction in human OA (22) and the cell-type specific role of TGFβ in OA, we evaluated the cartilage phenotype of TβRII$^{ocy-/-}$ mice to elucidate the role of osteocytic TGFβ signaling in joint homeostasis. When compared with control mice, TβRII$^{ocy-/-}$ mice had significantly increased Mankin scores in the whole joint and in the medial and lateral compartments, with a disruption of articular cartilage structure, loss of proteoglycan staining, increased hypertrophic chondrocytes, and increased subchondral bone thickness (Figure 1F–1I). TβRII$^{ocy-/-}$ mice did not have a statistically significant increase in OARSI score (data not shown).

Although female TβRII$^{ocy-/-}$ mice also had reduced osteocytic expression of TβRII in the subchondral bone by 45% (Figure 2A, 2B), for canalicular length and Mankin score, female TβRII$^{ocy-/-}$ mice were indistinguishable from female controls (Figure 2C–2G). Therefore, phenotypic differences in male and female TβRII$^{ocy-/-}$ mice are not the result of differences in reduction of osteocytic TβRII, and the requirement of osteocytic TβRII for subchondral bone lacunocanalicular network maintenance and articular cartilage homeostasis is sexually dimorphic.

Increased subchondral bone plate thickness in male, but not female, TβRII$^{ocy-/-}$ joints

Osteocytic defects in TGFβ signaling could drive cartilage degeneration in male mice by disrupting the mechanical or biological environment of the subchondral bone. Changes in joint mechanics and subchondral bone plate (SBP) thickness are closely linked to OA development, suggesting that disruption of subchondral bone mechanics exacerbates cartilage degeneration (2, 39). To examine the relationship between osteocytic TβRII, subchondral bone mechanics, and cartilage degeneration, we quantified SBP thickness in male and female mice, focusing on the load-bearing posterior regions of control and TβRII$^{ocy-/-}$ distal femora (7). We found that the SBP of male TβRII$^{ocy-/-}$ mice is significantly thicker than in control mice on both the lateral and medial condyles (Figure 3A, 3B). The load-bearing femoral SBP thickness of female TβRII$^{ocy-/-}$ mice, however, does not significantly differ from female controls (Figure 3F, 3G). Coupled with the sex-specific effect of osteocytic TGFβ signaling on the canalicular network and SBP thickness in the bone, the sexual dimorphism in OA raises the possibility that altered joint mechanics in male TβRII$^{ocy-/-}$ mice leads to cartilage degeneration, while female TβRII$^{ocy-/-}$ mice have relatively normal joint mechanics and therefore healthy cartilage.

Coupled deregulation of sclerostin expression, SBP thickness, and cartilage homeostasis

Sclerostin is a negative regulator of bone formation, and TGFβ regulates load-dependent bone formation in a sclerostin-dependent manner (32, 40). We sought to determine if SBP sclerostin expression is sensitive to osteocytic TGFβ signaling, and furthermore, if this regulation is sexually dimorphic. Sclerostin was not detected in chondrocytes or articular cartilage in any condition (Figure 3C, 3H, 4B). Sclerostin expression in male TβRII$^{ocy-/-}$ SBP was significantly increased when compared with male controls (Figure 3C–3E), corresponding to the increased SBP thickness observed in TβRII$^{ocy-/-}$ mice. We previously observed elevated sclerostin levels in male mice expressing dominant negative TβRII under the control of the osteocalcin promoter (32), and we find the same to be true in male mice with an osteocytic ablation of TβRII. However, the female SBP showed no genotype-dependent difference in sclerostin expression (Figure 3H–3J), indicating that SBP sclerostin expression in TβRII$^{ocy-/-}$ mice is also sexually dimorphic. Thus, we observe a close relationship among cartilage degeneration, SBP thickness, and deregulated sclerostin expression; in male TβRII$^{ocy-/-}$ mice, genotype-dependent increases in cartilage degeneration colocalize with SBP thickening and excessive sclerostin, whereas in female TβRII$^{ocy-/-}$ mice, none of these outcomes differ from female controls. The extent to which these structural or biological changes in subchondral bone drive OA is unclear.

Osteocytic TGFβ signaling is required for injury-induced changes in subchondral bone and sclerostin expression

Given the need to clarify the relationship between OA progression and the changes in SBP thickness and sclerostin expression in TβRII$^{ocy-/-}$ mice, and the extent to which these may be mechanoregulated, we implemented an OA model in which a meniscal/ligamentous injury (MLI) preferentially disrupts the mechanical environment of the medial joint. MLI of control mice significantly increased SBP thickness, subchondral bone volume, and SBP sclerostin expression in the medial joint but elicited a more modest increase in SBP thickness on the lateral side (Figure 4). Importantly, MLI did not affect any of these parameters on either the 'loaded' medial side or the lateral side of the TβRII$^{ocy-/-}$ subchondral bone, indicating that injury-induced changes in subchondral bone require osteocytic TGFβ signaling (Figure 4E, 4H, 4K). Furthermore, on the medial side, apparent genotype-dependent differences in subchondral bone volume and sclerostin expression in sham mice disappeared following MLI (Figure 4F, 4I). Together with prior evidence implicating TGFβ in the anabolic response of bone to mechanical load (32), these data reveal that osteocytic TGFβ signaling is required for mechanosensitive changes in subchondral bone formation and sclerostin expression.

Increased cartilage degeneration in injured male TβRII$^{ocy-/-}$ mice

Compartmental evaluation of OA severity in this medial injury model allows dissection of mechanisms of joint crosstalk. Injury further exacerbates joint degeneration in TβRII$^{ocy-/-}$ mice compared with injured control mice, resulting in a significantly increased total Mankin score due to more severe disruption of the articular cartilage structure, loss of proteoglycans, and increased hypertrophic chondrocytes (Figure 5A, 5B). Compartmental analysis reveals that the increased Mankin score in injured TβRII$^{ocy-/-}$ joints results from increased cartilage degeneration on the uninjured lateral side of the TβRII$^{ocy-/-}$ joints relative to controls (Figure 5D). Importantly, on the injured medial side, the effect of MLI on cartilage in the control and TβRII$^{ocy-/-}$ mice is indistinguishable (Figure 5C). Thus, on the injured medial side, cartilage degeneration correlates with increased subchondral bone and sclerostin levels, independently of genotype. On the uninjured lateral side, where the mechanical environment is less affected, we observe worsened cartilage degeneration in TβRII$^{ocy-/-}$ mice, similar to that observed in the uninjured TβRII$^{ocy-/-}$ mice (Figure 1). Overall, independent of genotype, sex, or injury, increased SBP thickness corresponds spatially to cartilage degeneration. These findings suggest a critical role for osteocytic TGFβ signaling in controlling the SBP response to mechanical changes with injury.

Interestingly, our data suggest that osteocytic TGFβ signaling plays a bidirectional role in response to injury. Following injury, osteocytic TβRII expression in control subchondral bone is indistinguishable from TβRII$^{ocy-/-}$ mice, resulting in an injury-dependent decrease ($p=0.051$) in osteocytic TβRII expression in control mice (Figure 6A, 6B), further implicating osteocytic TGFβ signaling as key in the mechanosensitive response to injury. We examined possible mechanisms that could contribute to the more severe phenotype in male TβRII$^{ocy-/-}$ joints First, our findings suggest that the worsened cartilage phenotype on the lateral side in TβRII$^{ocy-/-}$ mice with MLI (Figure 5D) is due, at least in part, to the underlying increased SBP thickness, subchondral bone volume, and SBP sclerostin levels

prior to injury (Figure 4D, 4G, 4J). Second, changes in SBP thickness are insufficient to explain why injured TβRII$^{ocy-/-}$ mice exhibit more cartilage degeneration than sham TβRII$^{ocy-/-}$ mice (Figure 5B). Indeed, TβRII$^{ocy-/-}$ mice were insensitive to injury-induced changes in SBP thickness, subchondral bone volume, or sclerostin levels (Figure 4C–4K), indicating that other bone-independent factors with injury, such as inflammation or increased direct loading on the cartilage with meniscectomy, worsen cartilage degeneration in injured TβRII$^{ocy-/-}$ mice. We additionally observe a number of genotype-dependent differences that may participate. The expected genotype-dependent reduction in canalicular length was lost in the context of MLI (Figure 6C, 6D). Finally, we detect qualitative genotype-dependent differences in shape of the femoral condyles in TβRII$^{ocy-/-}$ mice, which were apparent in both male and female TβRII$^{ocy-/-}$ mice (Supplemental Figure 1C, 1F).

Discussion

In this study, we show that loss of osteocytic TGFβ signaling plays a causal role in articular cartilage degeneration through its spatial control of subchondral bone. Using an established mouse model of osteocyte-specific ablation of TβRII (23), we observed a close relationship among cartilage degeneration, SBP thickening, and osteocytic sclerostin upregulation in male TβRII$^{ocy-/-}$ mice and injured control mice, which additionally showed an injury-dependent decrease in osteocytic TβRII. On the contrary, female TβRII$^{ocy-/-}$ mice do not show these differences, indicating a sex-specific role for osteocytic TGFβ signaling in OA. With injury-induced changes in joint mechanics, control mice increase SBP thickness and sclerostin expression in spatial association with cartilage degeneration and repress osteocytic TβRII within the subchondral bone. Without osteocytic TβRII, however, injured TβRII$^{ocy-/-}$ mice do not increase SBP thickness and sclerostin expression, suggesting that SBP mechanosensation requires osteocytic TGFβ signaling. Overall, we find that increased SBP thickness and sclerostin expression, whether by loss of osteocytic TGFβ signaling or by medial injury, drives cartilage degeneration. Together, this work provides new insight into the factors driving changes in SBP thickness during joint degeneration, identifying osteocytes as potential targets for OA therapeutics.

Bone quality (41, 42) and OA (43, 44) show sex-specific differences in humans and mice. OA is more prevalent in women than in men, particularly after menopause, demonstrating a need to better understand the sex-specific pathogenesis of OA (44). We have recently shown that osteocytic TGFβ signaling induces PLR in a sex-specific manner (28). While male TβRII$^{ocy-/-}$ mice demonstrate hallmarks of suppressed PLR in the cortical bone, including blunted canalicular networks, reduced expression of PLR enzymes, and defective bone quality, PLR and bone quality in female TβRII$^{ocy-/-}$ mice remain intact (28). This set of observations remains true in this study, where 16-week-old male TβRII$^{ocy-/-}$ mice showed a disruption of the subchondral bone canalicular network, increased SBP thickness, and signs of worsened joint degeneration while female TβRII$^{ocy-/-}$ mice, did not, demonstrating that the sexually dimorphic role of osteocytic TGFβ signaling extends to the joint. These findings are consistent with the idea that altered mechanics at the SBP lead to cartilage degeneration. However, female TβRII$^{ocy-/-}$ joints were not entirely normal. Both male and female TβRII$^{ocy-/-}$ joints show qualitative shape differences of the femoral condyle, including a marked thickening of the SBP in the anterior region and an apparent rounding

of the condyle, as well as increased SBP thickness in the relatively unloaded anterior region of the femoral condyle (Supplemental Figure 1). These differences in female TβRII$^{ocy-/-}$ joints appear insufficient to affect joint degeneration at this time point, and further work is needed to understand the injury-induced mechanosensitive response in osteocytes in female TβRII$^{ocy-/-}$ mice. Osteocytes emerge as important regulators of SBP thickness and joint shape, and female TβRII$^{ocy-/-}$ mice are thus able to maintain joint health in the absence of osteocytic TGFβ signaling.

SBP thickness changes over the course of OA progression, and the spatial association of SBP thickening with cartilage degeneration is a hallmark of late-stage OA (1–7). Additionally, TGFβ signaling participates in mechanoregulation of the skeleton (29–32), which, in the context of osteocytic TGFβ signaling, could impact the response of the SBP to changes in joint mechanics. Using TβRII$^{ocy-/-}$ mice, we find evidence that the mechanoresponse to injury at the SBP requires osteocytic TGFβ signaling. Unlike injured control mice, injured TβRII$^{ocy-/-}$ mice are insensitive to injury-induced changes in SBP thickness, subchondral bone volume, and SBP sclerostin expression. Notably, injured TβRII$^{ocy-/-}$ mice still have worsened cartilage degeneration, which was primarily driven by an increase in OA score on the uninjured lateral tibia (Figure 5D). This suggests that the underlying increase in SBP thickness on the ‘uninjured’ lateral side of TβRII$^{ocy-/-}$ mice is sufficient to disrupt the normal mechanical environment of the joint and drives cartilage degeneration. Notably, although we previously observed an injury-dependent disruption of the subchondral bone lacunocanalicular network in a different mouse model of PLR suppression (22), we do not observe an injury-dependent decrease in canalicular length in this study, possibly due to genetic differences in these mouse models or selected regions of interest. Together, these findings indicate that osteocytic TGFβ signaling is critical for the spatial association between cartilage degeneration and SBP thickness in late-stage OA and the mechanosensitive response to injury.

In contrast to previous studies, we observed an increase in sclerostin expression in the setting of increased SBP thickness and cartilage degeneration. Others observe an inverse relationship between sclerostin levels and OA severity in humans (45) and a repression of sclerostin with increased SBP thickness in late-stage OA in mice (7). Because sclerostin expression is induced by TGFβ (32, 40), repressed in response to load (46), and stimulates PLR (27), we expected to observe decreased sclerostin expression in TβRII$^{ocy-/-}$ mice and injured control mice. Instead, we surprisingly observed a significant increase in sclerostin-positive osteocytes in all cases with increased SBP thickness, which was spatially confined to the SBP and not the axial femur (Supplemental Figure 2). One possible explanation for the elevated sclerostin is that increased SBP thickness reduces osteocyte sensitivity to equivalent loads. Additionally, sclerostin upregulation may indicate a compensation for defective PLR due to loss of osteocytic TβRII (27) or altered dynamics of osteocytic differentiation. Taken together, our study and others (7) demonstrate that coordinated regulation of sclerostin and the SBP is critical in joint homeostasis, which is likely dynamic over the course of OA progression. While sclerostin has been studied in the context of OA in mice and rats, either through sclerostin inhibition or treating with recombinant Sost protein (47, 48), the extent to which sclerostin exacerbates the joint phenotype remains unclear. Given the current clinical use of romosozumab, an anti-sclerostin antibody, for human

osteoporosis (49, 50), further work is needed to resolve the mechanistic role of sclerostin in the joint and OA.

Limitations of this study include the use of a mouse model with constitutive ablation of osteocytic TβRII, which confounds the observed TβRII$^{ocy-/-}$ joint phenotype with the effects of TβRII in joint development. While this work describes a correlation among osteocytic TGFβ signaling, SBP thickness, and SBP sclerostin expression, further work is needed to establish a causal role for SBP sclerostin in the cartilage phenotype. Though uninjured TβRII$^{ocy-/-}$ mice have an increased Mankin score when compared with uninjured controls, sham-operated TβRII$^{ocy-/-}$ mice do not have a genotype-dependent increase in cartilage degeneration, suggesting that other factors impact joint homeostasis, such as inflammation following incision in the sham-operated groups. Finally, additional work is needed to elucidate the mechanisms by which joint injury represses subchondral bone osteocytic TβRII expression.

In summary, our findings demonstrate that mechanoregulation of bone requires osteocytic TGFβ signaling to regulate sclerostin and SBP thickness and maintain cartilage homeostasis (Figure 6E). We observed increased sclerostin expression at the SBP and exacerbated joint degeneration in settings with increased SBP thickness, such as in male TβRII$^{ocy-/-}$ mice or on the medial side of injured control mice, but not in female TβRII$^{ocy-/-}$ mice. These findings suggest that osteocyte-intrinsic defects in TGFβ signaling can play a contributory role in OA progression, further implicating osteocytes as being a key participant of healthy joint homeostasis through bone-cartilage crosstalk.

Supplementary Material

Refer to Web version on PubMed Central for supplementary material.

Acknowledgements

This research was supported by the National Institute of Dental and Craniofacial Research (R01 DE019284), the Department of Defense (OR130191), the National Science Foundation (1636331), the Read Research Foundation, the National Institute of General Medical Sciences (T32GM007618), and the UCSF Summer Research Training Program. The authors gratefully acknowledge Courtney Mazur and Jennifer Salinas for assistance with histological analysis.

References

1. Goldring SR, Goldring MB. Changes in the osteochondral unit during osteoarthritis: structure, function and cartilage-bone crosstalk. Nat Rev Rheumatol. 2016;12(11):632–44. [PubMed: 27652499]
2. Burr DB, Gallant MA. Bone remodelling in osteoarthritis. Nat Rev Rheumatol. 2012;8(11):665–73. [PubMed: 22868925]
3. Kuroki K, Cook CR, Cook JL. Subchondral bone changes in three different canine models of osteoarthritis. Osteoarthritis Cartilage. 2011;19(9):1142–9. [PubMed: 21736944]
4. Fahlgren A, Messner K, Aspenberg P. Meniscectomy leads to an early increase in subchondral bone plate thickness in the rabbit knee. Acta Orthop Scand. 2003;74(4):437–41. [PubMed: 14521295]
5. Benske J, Schunke M, Tillmann B. Subchondral bone formation in arthrosis. Polychrome labeling studies in mice. Acta Orthop Scand. 1988;59(5):536–41. [PubMed: 3055797]

6. Wu DD, Burr DB, Boyd RD, Radin EL. Bone and cartilage changes following experimental varus or valgus tibial angulation. J Orthop Res. 1990;8(4):572–85. [PubMed: 2355297]
7. Jia H, Ma X, Wei Y, Tong W, Tower RJ, Chandra A, et al. Loading-Induced Reduction in Sclerostin as a Mechanism of Subchondral Bone Plate Sclerosis in Mouse Knee Joints During Late-Stage Osteoarthritis. Arthritis Rheumatol. 2018;70(2):230–41. [PubMed: 29024567]
8. Grafe I, Yang T, Alexander S, Homan EP, Lietman C, Jiang MM, et al. Excessive transforming growth factor-beta signaling is a common mechanism in osteogenesis imperfecta. Nat Med. 2014;20(6):670–5. [PubMed: 24793237]
9. Chen CG, Thuillier D, Chin EN, Alliston T. Chondrocyte-intrinsic Smad3 represses Runx2-inducible matrix metalloproteinase 13 expression to maintain articular cartilage and prevent osteoarthritis. Arthritis Rheum. 2012;64(10):3278–89. [PubMed: 22674505]
10. Blaney Davidson EN, Remst DF, Vitters EL, van Beuningen HM, Blom AB, Goumans MJ, et al. Increase in ALK1/ALK5 ratio as a cause for elevated MMP-13 expression in osteoarthritis in humans and mice. J Immunol. 2009;182(12):7937–45. [PubMed: 19494318]
11. Wu Q, Kim KO, Sampson ER, Chen D, Awad H, O'Brien T, et al. Induction of an osteoarthritis-like phenotype and degradation of phosphorylated Smad3 by Smurf2 in transgenic mice. Arthritis Rheum. 2008;58(10):3132–44. [PubMed: 18821706]
12. Mohammad KS, Chen CG, Balooch G, Stebbins E, McKenna CR, Davis H, et al. Pharmacologic inhibition of the TGF-beta type I receptor kinase has anabolic and anti-catabolic effects on bone. PLoS One. 2009;4(4):e5275. [PubMed: 19357790]
13. Chang JL, Brauer DS, Johnson J, Chen CG, Akil O, Balooch G, et al. Tissue-specific calibration of extracellular matrix material properties by transforming growth factor-beta and Runx2 in bone is required for hearing. EMBO Rep. 2010;11(10):765–71. [PubMed: 20847738]
14. Balooch G, Balooch M, Nalla RK, Schilling S, Filvaroff EH, Marshall GW, et al. TGF-beta regulates the mechanical properties and composition of bone matrix. Proc Natl Acad Sci U S A. 2005;102(52):18813–8. [PubMed: 16354837]
15. Alliston T Biological regulation of bone quality. Curr Osteoporos Rep. 2014;12(3):366–75. [PubMed: 24894149]
16. Valdes AM, Spector TD, Tamm A, Kisand K, Doherty SA, Dennison EM, et al. Genetic variation in the SMAD3 gene is associated with hip and knee osteoarthritis. Arthritis Rheum. 2010;62(8):2347–52. [PubMed: 20506137]
17. Serra R, Johnson M, Filvaroff EH, LaBorde J, Sheehan DM, Derynck R, et al. Expression of a truncated, kinase-defective TGF-beta type II receptor in mouse skeletal tissue promotes terminal chondrocyte differentiation and osteoarthritis. J Cell Biol. 1997;139(2):541–52. [PubMed: 9334355]
18. van de Laar IM, Oldenburg RA, Pals G, Roos-Hesselink JW, de Graaf BM, Verhagen JM, et al. Mutations in SMAD3 cause a syndromic form of aortic aneurysms and dissections with early-onset osteoarthritis. Nat Genet. 2011;43(2):121–6. [PubMed: 21217753]
19. Yang X, Chen L, Xu X, Li C, Huang C, Deng CX. TGF-beta/Smad3 signals repress chondrocyte hypertrophic differentiation and are required for maintaining articular cartilage. J Cell Biol. 2001;153(1):35–46. [PubMed: 11285272]
20. Xie L, Tintani F, Wang X, Li F, Zhen G, Qiu T, et al. Systemic neutralization of TGF-beta attenuates osteoarthritis. Ann N Y Acad Sci. 2016;1376(1):53–64. [PubMed: 26837060]
21. Zhen G, Wen C, Jia X, Li Y, Crane JL, Mears SC, et al. Inhibition of TGF-beta signaling in mesenchymal stem cells of subchondral bone attenuates osteoarthritis. Nat Med. 2013;19(6):704–12. [PubMed: 23685840]
22. Mazur CM, Woo JJ, Yee CS, Fields AJ, Acevedo C, Bailey KN, et al. Osteocyte dysfunction promotes osteoarthritis through MMP13-dependent suppression of subchondral bone homeostasis. Bone Res. 2019;7:34. [PubMed: 31700695]
23. Dole NS, Mazur CM, Acevedo C, Lopez JP, Monteiro DA, Fowler TW, et al. Osteocyte-Intrinsic TGF-beta Signaling Regulates Bone Quality through Perilacunar/Canalicular Remodeling. Cell Rep. 2017;21(9):2585–96. [PubMed: 29186693]
24. Bonewald LF. The amazing osteocyte. J Bone Miner Res. 2011;26(2):229–38. [PubMed: 21254230]

25. Qing H, Ardeshirpour L, Pajevic PD, Dusevich V, Jahn K, Kato S, et al. Demonstration of osteocytic perilacunar/canalicular remodeling in mice during lactation. J Bone Miner Res. 2012;27(5):1018–29. [PubMed: 22308018]
26. Jahn K, Kelkar S, Zhao H, Xie Y, Tiede-Lewis LM, Dusevich V, et al. Osteocytes Acidify Their Microenvironment in Response to PTHrP In Vitro and in Lactating Mice In Vivo. J Bone Miner Res. 2017;32(8):1761–72. [PubMed: 28470757]
27. Kogawa M, Wijenayaka AR, Ormsby RT, Thomas GP, Anderson PH, Bonewald LF, et al. Sclerostin regulates release of bone mineral by osteocytes by induction of carbonic anhydrase 2. J Bone Miner Res. 2013;28(12):2436–48. [PubMed: 23737439]
28. Dole NS, Yee CS, Mazur CM, Acevedo C, Alliston T. TGFbeta Regulation of Perilacunar/Canalicular Remodeling Is Sexually Dimorphic. J Bone Miner Res. 2020.
29. Rys JP, DuFort CC, Monteiro DA, Baird MA, Oses-Prieto JA, Chand S, et al. Discrete spatial organization of TGFbeta receptors couples receptor multimerization and signaling to cellular tension. Elife. 2015;4:e09300. [PubMed: 26652004]
30. Rys JP, Monteiro DA, Alliston T. Mechanobiology of TGFbeta signaling in the skeleton. Matrix Biol. 2016;52-54:413–25. [PubMed: 26877077]
31. Wipff PJ, Hinz B. Integrins and the activation of latent transforming growth factor beta1 - an intimate relationship. Eur J Cell Biol. 2008;87(8-9):601–15. [PubMed: 18342983]
32. Nguyen J, Tang SY, Nguyen D, Alliston T. Load regulates bone formation and Sclerostin expression through a TGFbeta-dependent mechanism. PLoS One. 2013;8(1):e53813. [PubMed: 23308287]
33. Kamekura S, Hoshi K, Shimoaka T, Chung U, Chikuda H, Yamada T, et al. Osteoarthritis development in novel experimental mouse models induced by knee joint instability. Osteoarthritis Cartilage. 2005;13(7):632–41. [PubMed: 15896985]
34. Fowler TW, Acevedo C, Mazur CM, Hall-Glenn F, Fields AJ, Bale HA, et al. Glucocorticoid suppression of osteocyte perilacunar remodeling is associated with subchondral bone degeneration in osteonecrosis. Sci Rep. 2017;7:44618. [PubMed: 28327602]
35. Ploton D, Menager M, Jeannesson P, Himber G, Pigeon F, Adnet JJ. Improvement in the staining and in the visualization of the argyrophilic proteins of the nucleolar organizer region at the optical level. Histochem J. 1986;18(1):5–14. [PubMed: 2423479]
36. Safranin O/Fast Green Stain for Cartilage. University of Rochester Center for Musculoskeletal Research. 2017.
37. Furman BD, Strand J, Hembree WC, Ward BD, Guilak F, Olson SA. Joint degeneration following closed intraarticular fracture in the mouse knee: a model of posttraumatic arthritis. J Orthop Res. 2007;25(5):578–92. [PubMed: 17266145]
38. Glasson SS, Chambers MG, Van Den Berg WB, Little CB. The OARSI histopathology initiative - recommendations for histological assessments of osteoarthritis in the mouse. Osteoarthritis Cartilage. 2010;18 Suppl 3:S17–23.
39. Felson DT. Osteoarthritis as a disease of mechanics. Osteoarthritis Cartilage. 2013;21(1):10–5. [PubMed: 23041436]
40. Loots GG, Keller H, Leupin O, Murugesh D, Collette NM, Genetos DC. TGF-beta regulates sclerostin expression via the ECR5 enhancer. Bone. 2012;50(3):663–9. [PubMed: 22155511]
41. Vashishth D, Gibson GJ, Fyhrie DP. Sexual dimorphism and age dependence of osteocyte lacunar density for human vertebral cancellous bone. Anat Rec A Discov Mol Cell Evol Biol. 2005;282(2):157–62. [PubMed: 15627986]
42. Tiede-Lewis LM, Xie Y, Hulbert MA, Campos R, Dallas MR, Dusevich V, et al. Degeneration of the osteocyte network in the C57BL/6 mouse model of aging. Aging (Albany NY). 2017;9(10):2190–208. [PubMed: 29074822]
43. Ma HL, Blanchet TJ, Peluso D, Hopkins B, Morris EA, Glasson SS. Osteoarthritis severity is sex dependent in a surgical mouse model. Osteoarthritis Cartilage. 2007;15(6):695–700. [PubMed: 17207643]
44. Srikanth VK, Fryer JL, Zhai G, Winzenberg TM, Hosmer D, Jones G. A meta-analysis of sex differences prevalence, incidence and severity of osteoarthritis. Osteoarthritis Cartilage. 2005;13(9):769–81. [PubMed: 15978850]

45. Wu L, Guo H, Sun K, Zhao X, Ma T, Jin Q. Sclerostin expression in the subchondral bone of patients with knee osteoarthritis. Int J Mol Med. 2016;38(5): 1395–402. [PubMed: 27665782]

46. Robling AG, Niziolek PJ, Baldridge LA, Condon KW, Allen MR, Alam I, et al. Mechanical stimulation of bone in vivo reduces osteocyte expression of Sost/sclerostin. J Biol Chem. 2008;283(9):5866–75. [PubMed: 18089564]

47. Roudier M, Li X, Niu QT, Pacheco E, Pretorius JK, Graham K, et al. Sclerostin is expressed in articular cartilage but loss or inhibition does not affect cartilage remodeling during aging or following mechanical injury. Arthritis Rheum. 2013;65(3):721–31. [PubMed: 23233270]

48. Chang JC, Christiansen BA, Murugesh DK, Sebastian A, Hum NR, Collette NM, et al. SOST/Sclerostin Improves Posttraumatic Osteoarthritis and Inhibits MMP2/3 Expression After Injury. J Bone Miner Res. 2018;33(6):1105–13. [PubMed: 29377313]

49. McClung MR. Romosozumab for the treatment of osteoporosis. Osteoporos Sarcopenia. 2018;4(1):11–5. [PubMed: 30775535]

50. Simpson EL, Martyn-St James M, Hamilton J, Wong R, Gittoes N, Selby P, et al. Clinical effectiveness of denosumab, raloxifene, romosozumab, and teriparatide for the prevention of osteoporotic fragility fractures: A systematic review and network meta-analysis. Bone. 2020;130:115081. [PubMed: 31626995]

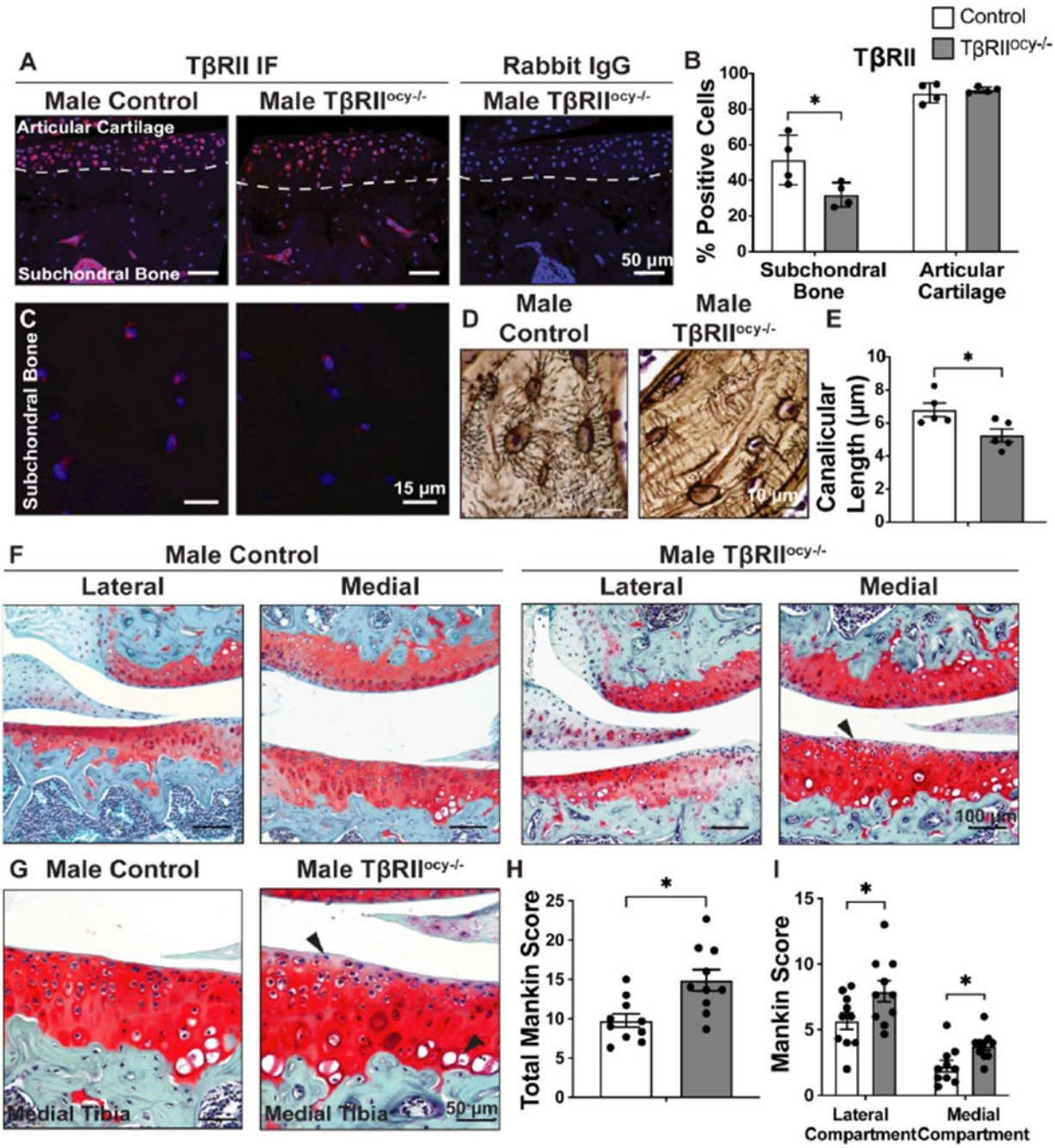

Figure 1: Osteocytic TGFβ signaling is required for canalicular network and articular cartilage homeostasis in 16-week-old male mice.

Immunofluorescence (IF) of TβRII shows a significant repression in subchondral bone osteocytes with no difference in expression in articular chondrocytes in male TβRII$^{ocy-/-}$ mice compared with control mice (A, scale bar = 50 μm, C, scale bar = 15 μm), demonstrating an osteocyte-specific loss of TβRII in TβRII$^{ocy-/-}$ mice (B, n = 4 mice per genotype). Lacunocanalicular networks of the subchondral bone are disrupted in male TβRII$^{ocy-/-}$ mice compared with control mice (Ploton Silver stain, D, scale bar = 10 μm), resulting in significantly decreased canalicular length (E, n = 5 mice per genotype). 16-week

old male TβRII$^{ocy-/-}$ mice have significantly increased Mankin scores in the whole joint (H, n = 10 mice per genotype) and the medial and lateral joint compartments (I, n = 10 mice per genotype) when compared with control mice (Safranin-O/Fast Green stain, F, scale bar = 100 μm, G, scale bar = 50 μm). Arrows denote proteoglycan loss and hypertrophic chondrocytes in TβRII$^{ocy-/-}$ medial tibia. Bar graphs represent mean ± SD (B) and mean ± SEM (E, H, I). *p<0.05 between genotypes by unpaired Students t test.

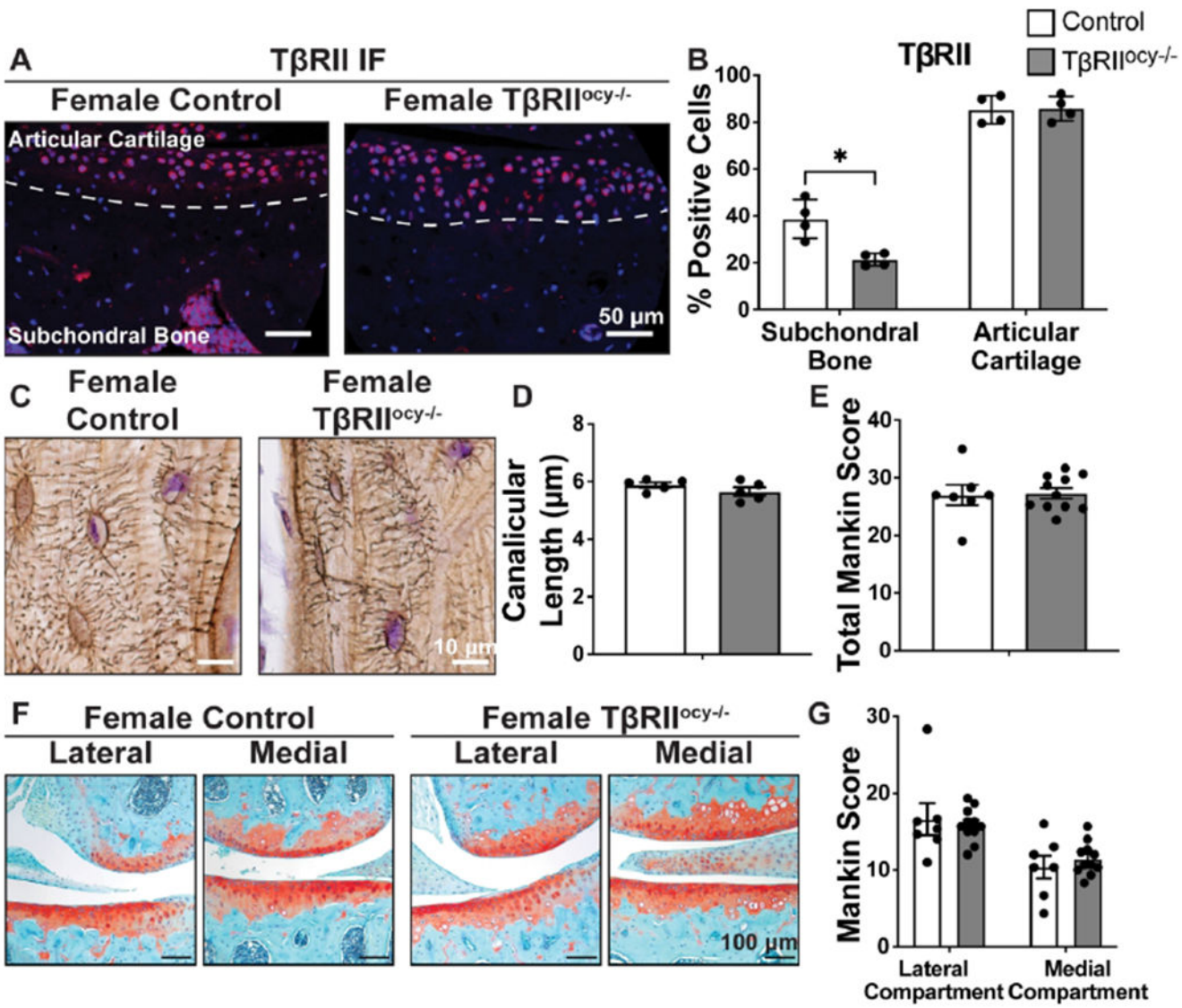

Figure 2: The requirement of osteocytic TβRII for canalicular network and articular cartilage homeostasis is sexually dimorphic.

Compared with female control mice, female TβRII$^{ocy-/-}$ mice demonstrate a repression of TβRII-positive osteocytes in the subchondral bone with no difference in TβRII expression in articular chondrocytes using immunofluorescence (IF) of TβRII (A, B, scale bar = 50 μm, n = 4 mice per genotype). Lacunocanalicular networks between female TβRII$^{ocy-/-}$ mice and female control mice are indistinguishable (Ploton Silver stain, C, scale bar = 10 μm), resulting in no difference in canalicular length (D, n = 5 mice per genotype). Female TβRII$^{ocy-/-}$ mice at 16 weeks of age show no differences in cartilage degeneration when compared with control mice (Safranin-O/Fast Green stain, F, scale bar = 100 μm), resulting in no difference in Mankin scores in the whole joint (E, n = 7-11 mice per genotype) or in the medial and lateral joint compartments (G, n = 7-11 mice per genotype). Bar graphs represent mean ± SD (B) and mean ± SEM (D, E, G). *p<0.05 between genotypes by unpaired Students t test.

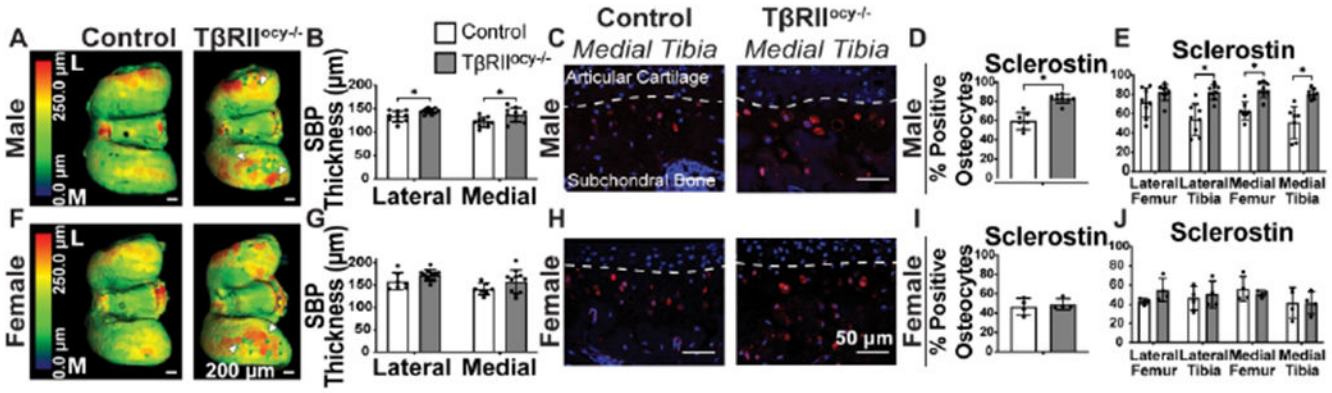

Figure 3: Subchondral bone plate thickness and sclerostin expression are increased in male, but not in female, TβRII$^{ocy-/-}$ mice.

Male TβRII$^{ocy-/-}$ femoral condyles have spatial differences, denoted by white arrows, in subchondral bone plate (SBP) thickness compared with male control mice (microCT thickness maps, A, scale bar = 200 μm), resulting in significantly higher SBP thickness in the medial and lateral condyles (B, n = 10 mice per genotype). SBP thickness in female TβRII$^{ocy-/-}$ mice is not significantly different from female control mice (F, G, scale bar = 200 μm, n = 7-11 mice per genotype). Immunofluorescence (IF) of sclerostin at the SBP is significantly increased in male TβRII$^{ocy-/-}$ mice compared with male control mice overall and in the lateral tibia, medial femur, and medial tibia joint quadrants specifically (C, D, E, scale bar = 50 μm, n = 8 mice per genotype). IF of sclerostin in female TβRII$^{ocy-/-}$ mice is indistinguishable from female control mice (H, scale bar = 50 μm), resulting in no significant differences in sclerostin expression overall or in each independent joint quadrant (I, J n = 4 mice per genotype). Bar graphs represent mean ± SD. *$p<0.05$ between genotypes by unpaired Students t test.

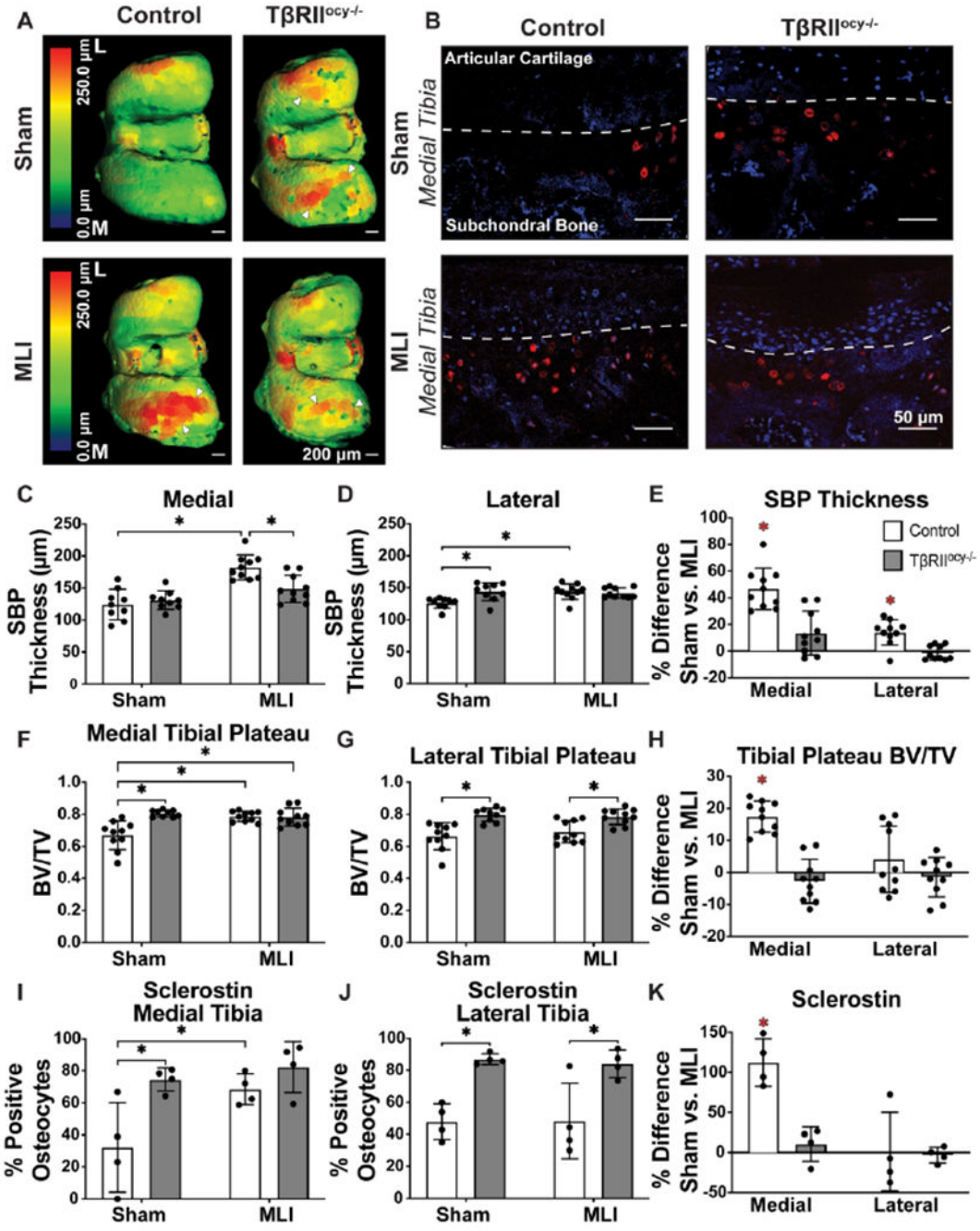

Figure 4: Osteocytic TβRII is critical for injury-induced changes in subchondral bone and sclerostin expression.

MicroCT thickness maps show spatial differences, denoted by white arrows, in subchondral bone plate (SBP) thickness of the femoral condyles (A, scale bar = 200 μm). Injury in control mice resulted in a significant increase in SBP thickness on the medial and lateral femoral condyles (C, D, n = 9-10 mice per group). Subchondral bone volume fraction (F, G, n = 9-10 mice per group) and immunofluorescence (IF) of sclerostin in the SBP (B, I, J, scale bar = 50 μm, n = 4 mice per group) reveal a genotype-dependent increase in sham mice in the medial and lateral tibia, and an injury-dependent increase in the medial tibia of control

mice. TβRII$^{ocy-/-}$ mice were insensitive to injury-induced changes in SBP thickness (E, n = 9-10 mice per group), subchondral bone volume fraction (H, n = 9-10 mice per group), and sclerostin expression (K, n = 4 mice per group). Bar graphs represent mean ± SD. *$p<0.05$ between groups by two-way ANOVA and Tukey post-hoc test.

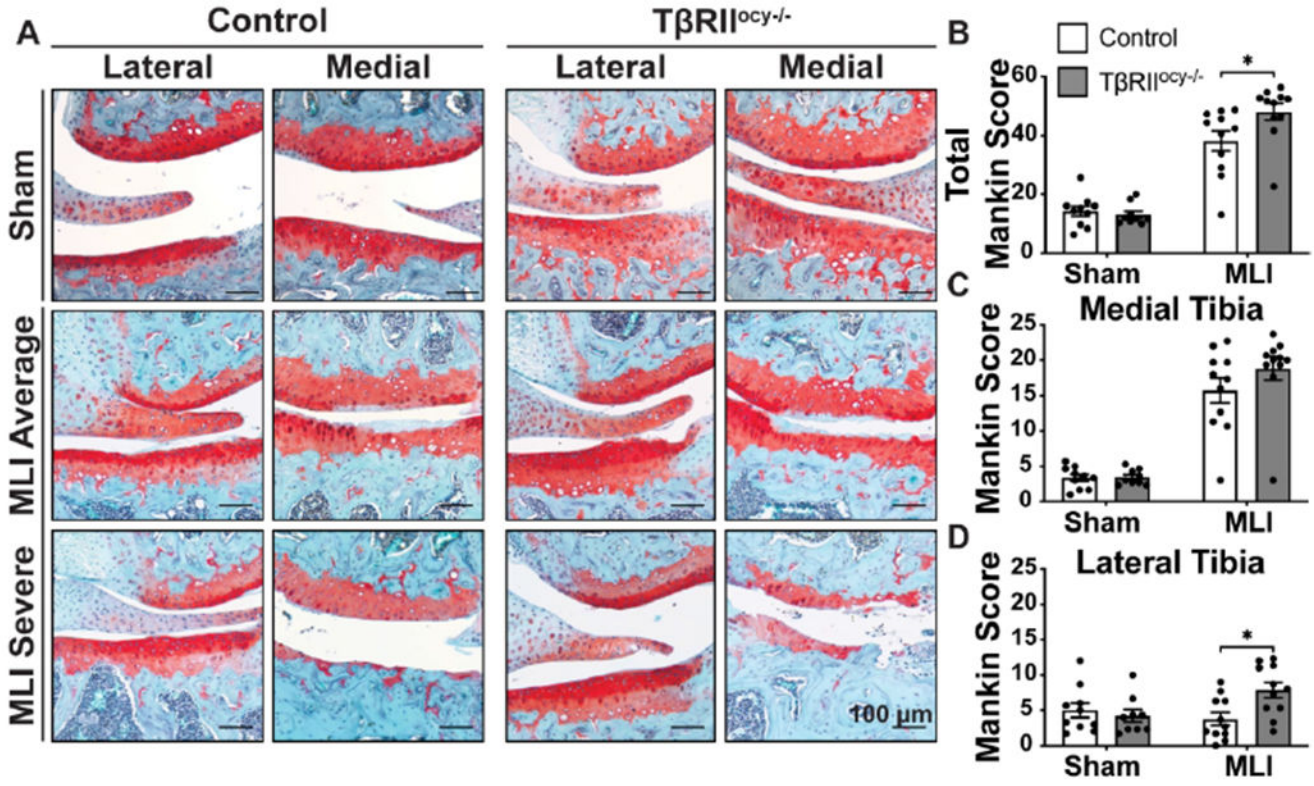

Figure 5: Loss of osteocytic TGFβ signaling exacerbates joint degeneration with injury.

Cartilage degeneration is worsened on the medial side with injury in TβRII$^{ocy-/-}$ and control mice, and injured TβRII$^{ocy-/-}$ mice have worsened OA phenotype compared with injured control mice (Safranin-O/Fast Green stain, A, scale bar = 100 μm), resulting in significantly higher whole joint Mankin score in injured TβRII$^{ocy-/-}$ mice compared with injured control mice. Medial injury increased total joint Mankin score (B, n = 9-11 mice per group) and medial tibia Mankin score (C, n = 9-11 mice per group) in control and TβRII$^{ocy-/-}$ mice when compared with respective sham controls. There was no difference between injured TβRII$^{ocy-/-}$ mice and injured control mice in the medial tibia (C, n = 9-11 mice per group), but significantly higher Mankin score in the lateral tibia of injured TβRII$^{ocy-/-}$ mice compared with injured control mice (D, n = 9-11 mice per group). Bar graphs represent mean ± SEM. *p<0.05 between groups by two-way ANOVA and Tukey post-hoc test.

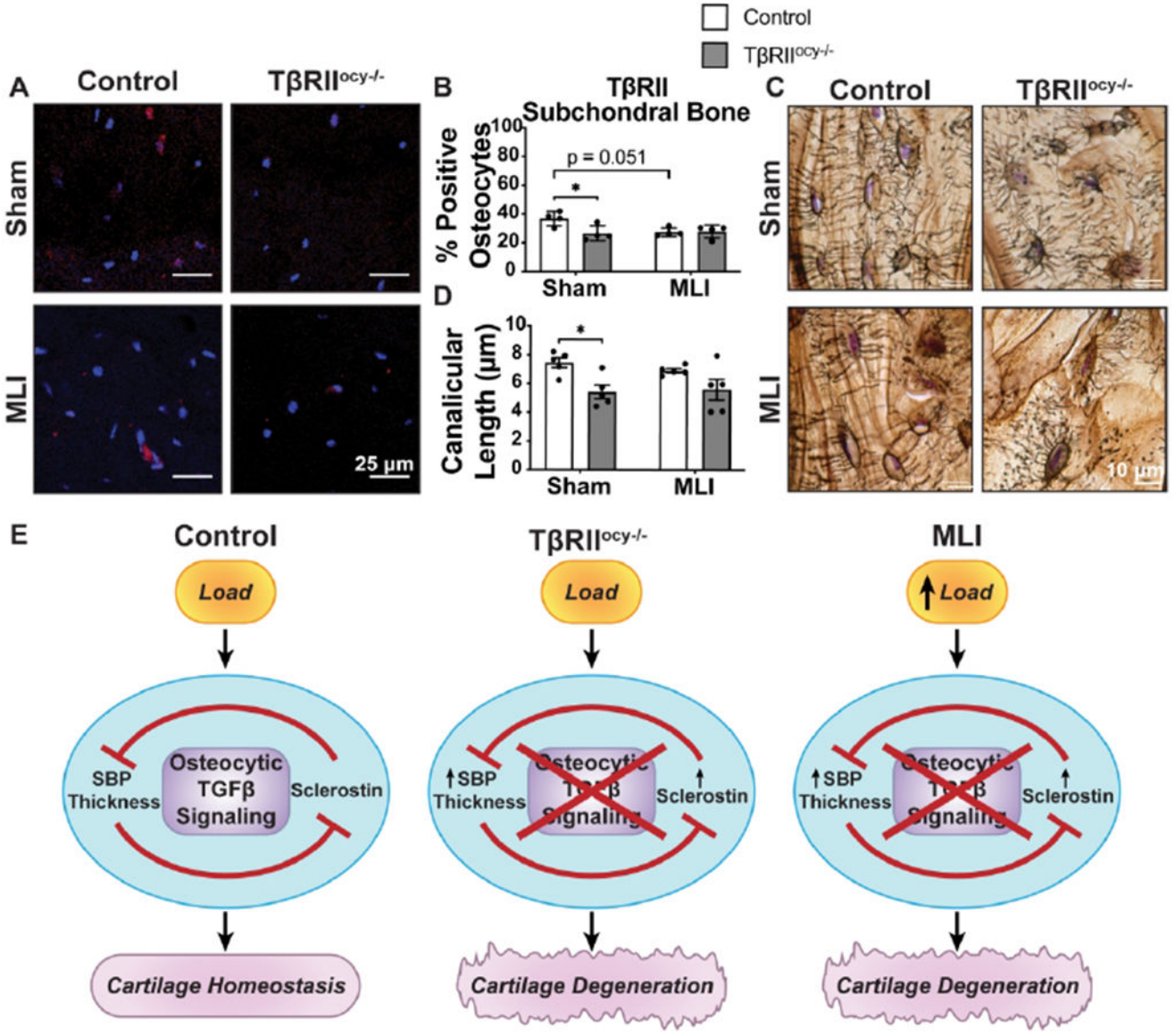

Figure 6: Injury represses osteocytic TGFβ signaling and diminishes genotype-dependent differences in canalicular length.

Compared with sham-operated control mice, sham-operated TβRII$^{ocy-/-}$ mice possess fewer TβRII-positive osteocytes in the subchondral bone using immunofluorescence (IF) of TβRII (A, B, scale bar = 25 μm, n = 4 mice per genotype). Injury eliminates this genotype-dependent difference, resulting in a decrease in TβRII-positive osteocytes in injured control mice when compared with sham-operated control mice (p=0.051). Lacunocanalicular networks in the subchondral bone are disrupted between sham-operated control and TβRII$^{ocy-/-}$ mice, but not between injured control and TβRII$^{ocy-/-}$ mice (Ploton Silver stain, C, scale bar = 10 μm), resulting in a significant decrease of canalicular length between sham groups, but not between injured groups (D, n = 5 mice per group). Bar graphs represent mean ± SD (B) and mean ± SEM (D). *p<0.05 between groups by two-way ANOVA and Tukey post-hoc test. Mechanosensitive function of bone requires osteocytic

TGFβ to regulate subchondral bone thickness (SBP) and sclerostin in a concerted manner to maintain joint homeostasis (E).